Vol. 78: 107–119, 2017
doi: 10.3354/ame01810

AQUATIC MICROBIAL ECOLOGY
Aquat Microb Ecol

Published online January 27

Distribution of the marine cyanobacteria *Trichodesmium* and their association with iron-rich particles in the South Atlantic Ocean

Mariana Bernardi Bif[1,*], João Sarkis Yunes[2]

[1]Rosenstiel School of Marine and Atmospheric Sciences, University of Miami, Miami, FL 33149, USA
[2]Laboratório de Cianobactérias e Ficotoxinas, Instituto de Oceanografia, Universidade Federal do Rio Grande, Rio Grande, RS 96203-900, Brazil

ABSTRACT: Members of the genus *Trichodesmium* are commonly found in nutrient-limited tropical and subtropical ocean basins due to their capacity to fix atmospheric nitrogen (N_2). However, N_2 fixation requires supplementary iron and phosphorus, which can potentially become limiting nutrients for the growth of *Trichodesmium*. In order to understand the ecology and distribution of *Trichodesmium* in a poorly studied region of the South Atlantic Ocean, we collected physical, chemical, and biological data from dense populations. Despite relatively low concentrations of phosphate (<0.35 µM), we found *Trichodesmium* throughout the region, with the northernmost stations having the highest abundances in the surface layer (>157 000 trichomes l^{-1}). Using light microscopy, mixtures of biogenic and lithogenic particles were found attached to the colonies; composition analysis revealed high concentrations of iron (12–29% of the average particle composition), phosphorus (1–3%), and zinc (1–5%). Particles from the southernmost stations were unique in their titanium composition (5–6%), which was considered a tracer for the regional input of sediments by the La Plata River plume. Bacteria were associated with some *Trichodesmium* colonies, suggesting particle dissolution and remineralization as a mechanism for increasing the availability of nutrients, thus facilitating N_2 fixation. This study provides new information about the distribution of *Trichodesmium* in the South Atlantic Ocean and its association with particles and bacteria as an adaptation for extra nutrient acquisition.

KEY WORDS: Iron uptake · Shelf slope · Scanning Electron Microscopy · Bacterial association · Phytoplankton ecology

INTRODUCTION

Species of the cyanobacterial genus *Trichodesmium* (Ehrenberg 1830), a marine member of the order Oscillatoriales, can be found in tropical and subtropical oceans, from coastal zones to large-scale gyres (Capone et al. 2005). Their cells are organized as trichomes that commonly form colonies with fusiform (tufts) or spherical (puffs) shapes that accumulate on the surface. Since their growth rate is low, these aggregations are often correlated with physical conditions, such as low winds and shallow mixed layers (LaRoche & Breitbarth 2005). The global distribution of *Trichodesmium* is well documented for the northern hemisphere, but the southern region remains understudied (Luo et al. 2012).

The genus is well known to fix atmospheric nitrogen (N_2) without the need for specialized cells, and can maintain the activity during photosynthesis (Carpenter & Price 1976). This has allowed *Trichodesmium* to colonize nitrogen-poor waters, where non-diazotroph growth is limited by the nutrient. N_2 fixation, however, is a highly energetic process that requires additional elements to support the nitrogenase activity, such as iron and phosphorus (Sañudo-Wilhelmy et al. 2001).

*Corresponding author: marianabif@gmail.com

Elemental iron is only bioavailable when dissolved or as organic-complexed species (Hutchins et al. 1999); nonetheless, *Trichodesmium* aggregates atmospheric particles to use as an additional source of dissolved iron. This behavior was first observed by scanning electron microscopy (SEM), where accumulations of Sahara dust were found between the trichomes (Rueter at al. 1992). Culture experiments further explained the aggregation of particles and iron uptake processes, where natural populations were maintained under controlled laboratory conditions and received artificial iron-enriched particle add-ons. The colonies were able to trap and transport these particles to a specific anoxic and reduced region, a microenvironment more suitable for iron dissolution (Paerl & Bebout 1992, Rubin et al. 2011). Associations between *Trichodesmium* and heterotrophic bacteria that are able to transform oxides into bioavailable species maximize the iron uptake (Roe et al. 2012); however, these associations were never observed together with particle aggregation. In the eastern North Atlantic, the constant input of iron-rich dust from the Sahara Desert supports persistent populations of *Trichodesmium*, where surface aggregations can be seen in satellite images (Tyrrell et al. 2003, Agawin et al. 2013, Fernández et al. 2013). Unfortunately, these environmental studies did not attempt to localize particles and bacteria associated with trichomes.

Trichodesmium maximize phosphorus uptake by incorporating both dissolved inorganic and organic species due to alkaline phosphatase activity (Sohm & Capone 2006). The evolution of gas vesicles, with high resistance to water pressure, has allowed vertical migration of *Trichodesmium* in the water column by varying the carbohydrate concentration inside the organelle that acts as a ballast (Villareal & Carpenter 2003). If migration occurs as a pattern in the environment, we can expect a vertical distribution of trichomes along the water column to reach the phosphocline. The particles attached to the colonies could be an additional source for phosphorus, although this has never been investigated.

Other elements important for metabolism, including nickel, vanadium, molybdenum, and zinc, are also related to nitrogen fixation, enzyme composition, and cellular protection against oxidative stress (Nuester et al. 2012, Ho 2013). Although much has been done to understand the role these trace metals play in living organisms, their biochemical role requires additional investigation.

The high biomass of *Trichodesmium* supports a large fraction of the new input of nitrogen in the oceans, especially in oligotrophic regions (Karl et al. 2002). *Trichodesmium* are considered to play a key role in the biogeochemical cycle and have been studied in detail around the globe. However, only a few studies have focused on the South Atlantic Ocean, leaving a gap of information on their distribution, taxonomy, and ecology. An excellent database that compiled global information about *Trichodesmium* and other diazotrophs reveals the lack of research in the South Atlantic (Luo et al. 2012). Biomass and nitrogen fixation measurements in the region, until now, are rare and restricted to open waters. On the Brazilian coast, the first study involving *Trichodesmium* was conducted by Sato et al. (1963) in the northeast region. They attributed health problems faced by the population of Tamandaré City to the accumulation of *Trichodesmium* on the shore; the inflammatory symptom was named 'Tamandaré fever.' Many unpublished and a few published data also suggest that the organism occurs in the northeast and southeast regions off the Brazilian coast (Carvalho et al. 2008, Monteiro et al. 2012).

The objective of this study was to characterize populations of *Trichodesmium* and provide insight into their ecology, spatial distribution, and biogeochemical role in the region. We focused on dense aggregations that occurred along the southern and southeastern Brazilian shelf slope, in the southwestern Atlantic Ocean. This work initially focused on: (1) the spatial and vertical distribution of the genus; (2) occurrence as single trichomes or as colonies; and (3) correlation with the nutrients in the environment. However, during observations under a microscope, we noticed the presence of particles attached to the colonies, prompting a detailed chemical analysis to verify particle composition. Therefore, this study coupled the distribution of *Trichodesmium* and inorganic nutrients in the region with chemical analysis of the associated particles. Finally, a potential source of iron-rich particles for the southernmost populations was identified. Furthermore, the images in this study support the evidence of an alternative source of nutrients for *Trichodesmium* in the ocean.

MATERIALS AND METHODS

Study area and physical parameters

The sampling area encompassed the Brazilian shelf slope, between 24 and 35° S, during 2 consecutive autumns. Stns 01 to 04 were sampled on 4–11 June 2013, and Stns 05 to 16 were sampled on 10–20 May 2014 on board the RV 'Atlântico Sul' (Universidade

Federal do Rio Grande [FURG], Brazil). Temperature and salinity measurements were obtained with a Sea-Bird® 911+ CTD (conductivity + temperature + depth) sensor. These data were used to classify the surface water masses (Möller et al. 2008) and calculate the mixed layer depth (MLD), which was determined from vertical density profiles ($\delta\rho/\delta z$). The upper 5 m were excluded due to noisy data (Table 1). The surface water masses are represented by stars in the map of the study area (Fig. 1), which was created using the free software ODV (Ocean Data View v.4; http://odv.awi.de) and GIMP (v.2.8.18; https://www.gimp.org).

Table 1. Sampling coordinates, sampling dates (mm/dd/yyyy), local depth, and mixed layer depth (MLD) at the stations (see Fig. 1)

Stn	Lat. (S)	Long. (W)	Date	Local depth (m)	MLD (m)
01	24° 16.6′	43° 22.2′	06/11/2013	692	45
02	25° 07.6′	44° 51.4′	06/08/2013	190	17
03	25° 48.8′	45° 04.2′	06/07/2013	1287	40
04	27° 6.4′	46° 24.7′	06/04/2013	830	80
05	28° 6.6′	48° 00.0′	05/20/2014	138	14
06	29° 22.9′	47° 08.8′	05/19/2014	1876	35
07	29° 26.0′	48° 24.8′	05/18/2014	140	35
08	30° 45.6′	48° 24′	05/17/2014	1505	80
09	31° 39.3′	49° 29.8′	05/15/2014	1816	43
10	31° 56.5′	49° 57.2′	05/14/2014	680	18
11	32° 12.9′	49° 41.1′	05/14/2014	1870	40
12	32° 18.2′	50° 06.6′	05/14/2014	806	40
13	32° 33.6′	50° 16.9′	05/13/2014	575	47
14	32° 55.3′	50° 17.6′	05/11/2014	676	15
15	33° 04.0′	50° 05.0′	05/12/2014	1166	20
16	33° 40.4′	51° 23.5′	05/10/2014	127	18

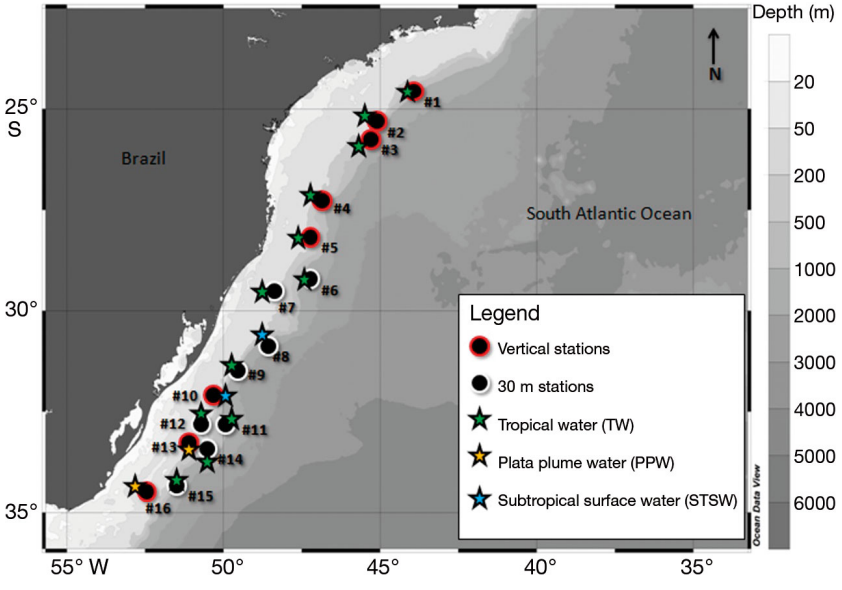

Fig. 1. South-southeastern Brazilian shelf slope, showing the sampling stations and surface water masses. Circles with red boarders represent stations where vertical profiles were collected

Nutrients

Water samples were collected using Niskin bottles coupled with messengers attached to the ship's cable from depths ranging from 15 m to a maximum of 140 m. All samples were then filtered with a cellulose filter (0.45 µm) and frozen in Falcon tubes for later analysis.

The nutrient analyses were performed using the following methods: total ammoniacal nitrogen (NH_4^+) (Koroleff 1972); nitrate (NO_3^-) (Aminot & Chaussepied 1983); nitrite (NO_2^-) (detection limit of 0.05 µM for each method); phosphate (PO_4^{2-}) and silicate (Si) (Aminot & Chaussepied 1983) (0.1 µM detection limit). Nutrients were analyzed via spectrophotometry using a handbook for chemical analyses that optimized the methods (Baumgarten et al. 2010). The sum of NH_4^+, NO_3^-, and NO_2^- concentrations was represented as dissolved inorganic nitrogen (DIN).

Biological parameters

Biological samples were collected using a closing ring plankton net (30 cm mouth diameter, 50 µm mesh size) with a messenger releasing mechanism. The net was also equipped with a ballast weight of approximately 8 kg that was used in order to maintain the net in vertical position in both descending (with the mouth open) and ascending movements. The mouth of the net was obstructed in established vertical hauls in order to collect layers of the water column (see Fig. S1 in the Supplement at www.int-res.com/articles/suppl/a078p107_supp.pdf). The samples were then preserved in 4% buffered formaldehyde.

During the first cruise, vertical layers at different depths were sampled using the net, only when *Trichodesmium* aggregations at the surface were visible to the naked eye. On the second cruise, additional samples were collected from the layer between 0 and 30 m depth independent of visible aggregations. The vertical layers were collected from the

surface to a maximum depth of 200 m. Sampling was usually conducted under suitable weather conditions, such as clear sky and calm seas, minimizing the angle between the net and the ship.

The abundance of *Trichodesmium* (Komárek & Anagnostidis 2007) was evaluated following the method of Utermöhl (1958). Briefly, subsamples were acidified with acetic acid (4%) in order to disrupt the gas vesicles and promote complete sedimentation of cells in the slide (Cronberg et al. 2003). They were then placed into sedimentation chambers with 10, 25, or 50 ml cylinders, chosen according to the concentration of cells from the original sample. The samples were allowed to settle for 24 to 48 h, depending on the volume of the chamber, and the trichomes were visualized under an inverted microscope (Zeiss Axiovert A1) coupled with a camera for image acquisition (AxioCam MRc) and optional UV light (UV fs09 ph1-04). The images were manipulated using the free software AxioVs40x64 (v. 4.9 1.0) and GIMP.

The abundance of trichomes was estimated by taking into consideration the volume of water filtered by the net that was concentrated into 200 ml amber vials and the volume of the cylinder + sedimentation chamber used by the Utermöhl method. Since the organism was commonly found in colonies, these colonies were also counted and distinguished between puffs and tufts. The average number of trichomes from each colony was estimated, based on the literature, as 200 trichomes colony^{-1} (Carpenter 1983). The abundance of *Trichodesmium* is shown in 4 different ways: (1) single trichomes l^{-1} (only free trichomes); (2 and 3) tufts and puffs (colonies of different shapes) l^{-1}; and (4) total trichomes l^{-1} (total trichomes l^{-1} = 200 × number of colonies + number of single trichomes). The vertical depth layers are represented as the abundance for each of the 4 features per depth range.

Chemical analysis of the particles

The particles attached to the colonies were analyzed by scanning electron microscope (SEM; JEOL 6060 LV) coupled with an energy-dispersive X-ray spectroscope (EDS) at a fixed voltage of 15 kV. For this analysis, representative stations were selected and prepared in replicates according to the number of colonies, location (southern, central, and northern samples), and water mass influence. The sediments were randomly analyzed by EDS and compiled in a database with *n* scans. This technique provided qualitative information about the chemical composition of the particles, and the result is shown as the contribution, in percentage, of each element among the total elements that compose the targeted particle.

SEM analysis was performed following the described preparation process. Initially, 5 to 10 ml of every replicate were filtered using a nuclepore filter (0.05 µm pore size) in order to concentrate enough biological material without clogging. The filter was then covered by another filter, washed 3 times with Milli-Q water to remove salts, and successively washed with increasing concentrations of ethanol solution for dehydration (5, 25, 50, 75, 95, and 100%; Association of European Marine Biological Laboratories). The samples were transported to the Centro de Microscopia Eletrônica da Zona Sul (CEME-Sul) facility at FURG for CO_2 critical point drying preparation (Tousimis Autosamdri®, model 815). This method substitutes the ethanol content in the cells with carbonic gas by exposing the filters to a controlled high temperature and pressure. The process dehydrates the cells while avoiding any cell surface tension, and provides a better and more realistic visualization of the sample. The last preparation step consisted of a metallic evolvement of the samples with gold (Denton Vacuum, Dorsk V). Finally, the filter membranes were positioned on stubs for observation.

Statistics

We conducted multivariate analyses using the abundance of *Trichodesmium* in the surface layer (0–30 m). The contribution of single trichomes and colonies to the total abundance for each station, and how similar these stations were, were calculated by similarity percentage analysis (SIMPER; Clarke 1993). In order to verify any spatial pattern in the trichomes/tufts/puffs proportions between the stations, we used a statistical non-metric multidimensional scaling (nMDS) analysis with dissimilarity matrix based on the non-metric Bray-Curtis index (Bray & Curtis 1957). An analysis of similarities (ANOSIM) was also applied (Clarke 1993) to verify possible differences among the groups based on their Bonferroni-corrected p-values. These analyses were performed using the free software PAST (v.1.81) (Hammer et al. 2008). The correlation between the numbers of colonies to the total trichomes for each station, using the data from all depths, was calculated using ODV software. The compositions of several particles were analyzed by SEM coupled with EDS, and resulting percentages of elements for each specific particle were averaged for each station. The results are presented as the average contribution of elements at each station.

RESULTS

Area of study, *Trichodesmium* abundance, and distribution of nutrients at the surface

Fig. 1 shows the surface water masses at each station. The region was under the influence of Tropical Water (TW, S < 36, T > 22.3°C), Plata Plume Water (PPW, S < 33.5, T ≤ 20.9°C), and Sub-Tropical Shelf Water (STSW, 33.5 < S < 35.5, T = 20.7°C).

Microscopy analysis showed a clear distinction between the tuft- and puff-shaped colonies that contributed significantly to the total of trichomes in the stations. Table 2 provides information about the abundance of *Trichodesmium* at the surface, categorized as single trichomes, colonies, and the sum of both (as total trichomes l^{-1}). *Trichodesmium* abundance was highest at the surface, especially in the 4 northernmost samples, reaching >157 000 trichomes l^{-1} (Table 2). Stns 10 and 11 had concentrations of >8000 trichomes l^{-1}, when the number of trichomes could be seen by the naked eye. Tuft and puff colonies were also high at those stations; the maximum concentration of tufts was 15 380 colonies l^{-1} at Stn 02, and the maximum of puffs was 8185 colonies l^{-1} at Stn 03. The concentrations of nutrients collected at 15 m depth are also shown in Table 2. Phosphate, DIN, and silicate concentrations were low at all stations. N:P ratios were lower than the Redfield ratio (16:1) at the surface, except for Stn 04 (16:1). The concentration of PO_4^{3-} was less than 0.35 µM, while the total ammoniacal nitrogen, nitrate, and nitrite concentrations were <1 µM individually and ≤1.5 µM as DIN.

The abundance of *Trichodesmium* at the surface is also shown in a surface plot (Fig. 2). The northern stations (Stns 01–04) contained the highest numbers of trichomes and colonies, by orders of magnitude more than the southern stations. As a consequence, the abundance in the southern region cannot be observed in detail in the map. Fig. 3 shows the surface distribution of inorganic nutrients, as well as the N:P ratios.

Statistical analyses were performed in order to evaluate the relative contribution of the colonies and single trichomes to the total trichomes at the surface. The nMDS analysis organized the stations into 3 distinct groups (A, B, and C; Fig. 4), based on the major contribution of puffs (Group A), tufts (Group B), and single trichomes (Group C) to the total abundance of *Trichodesmium*. ANOSIM found significant differences between these 3 groups based on Bonferroni-corrected p-values, which were <0.05 for all combinations. A SIMPER analysis was also carried out to calculate the average dissimilarities between the groups. The results showed 61.9% dissimilarity for puff- versus tuft-dominated groups, 67.1% dissimilarity for puff- versus single trichome-dominated, and 70.3% dissimilarity for tuft- versus single trichome-dominated.

Vertical distribution of *Trichodesmium* and nutrients

The distributions of total trichomes (number of colonies × 200 + single trichomes, as trichomes l^{-1}), free single trichomes l^{-1}, and colonies l^{-1} at different

Table 2. Abundance of trichomes or colonies (0–30 m depth) and concentration of nutrients at 15 m for each station (see Fig. 1). DIN: dissolved inorganic nitrogen

Stn	*Trichodesmium* abundance (trichomes or colonies l^{-1})				Nutrient concentration (µM)			
	Single trichomes	Tufts	Puffs	Total	PO_4^{-2}	DIN	Si	N:P
01	47151	1758	2598	918351	0.1	0.67		6.68
02	52325	15380	6385	4405325	0.12	1.16		9.67
03	213731	1444	8185	2139531	0.13	1.05		8.08
04	9816	84	654	157416	0.06	0.97		16.17
05	1180	0	0	1180	0	0	12.15	0
06	63	1	0	263	0	0.65	3.93	0
07	4	0	0	4	0.26	1.45	18.69	5.58
08	13	0	0	13	0	0.03	1.31	0
09	336	2	1	936	0	0.59	0.75	0
10	1385	24	10	8185	0	0.12	0	0
11	967	125	3	26567	0	0	2.06	0
12	26	0	0	26	0	0	3.45	0
13	1500	2	3	2500	0.21	0.7	19.8	3.4
14	338	1	3	1138	0.19	0.2	4.86	1.05
15	61	2	0	461	0.32	0	3.55	0
16	144	0	0	144	0.32	0	3.93	0

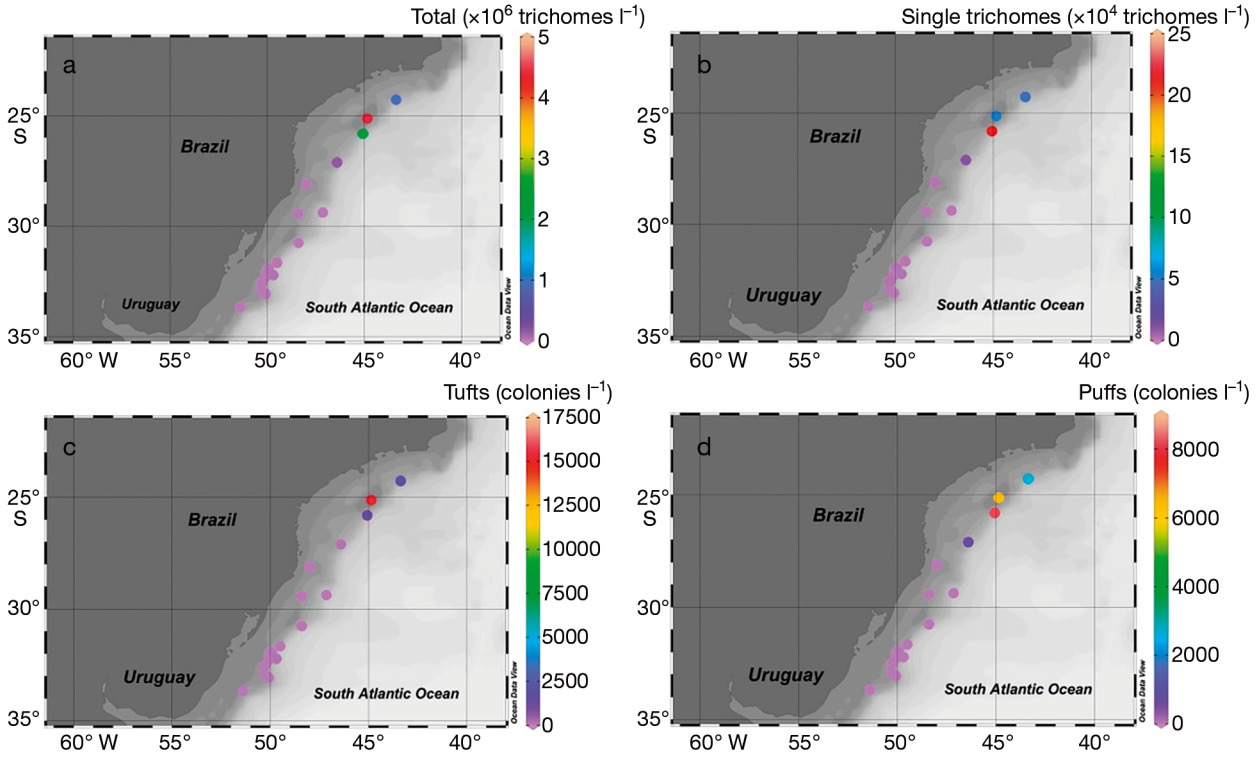

Fig. 2. Abundance of *Trichodesmium* at the surface in the South Atlantic Ocean, shown as (a) total trichomes l^{-1}, (b) single trichomes l^{-1}, (c) tuft-shaped colonies l^{-1}, and (d) puff-shaped colonies l^{-1}

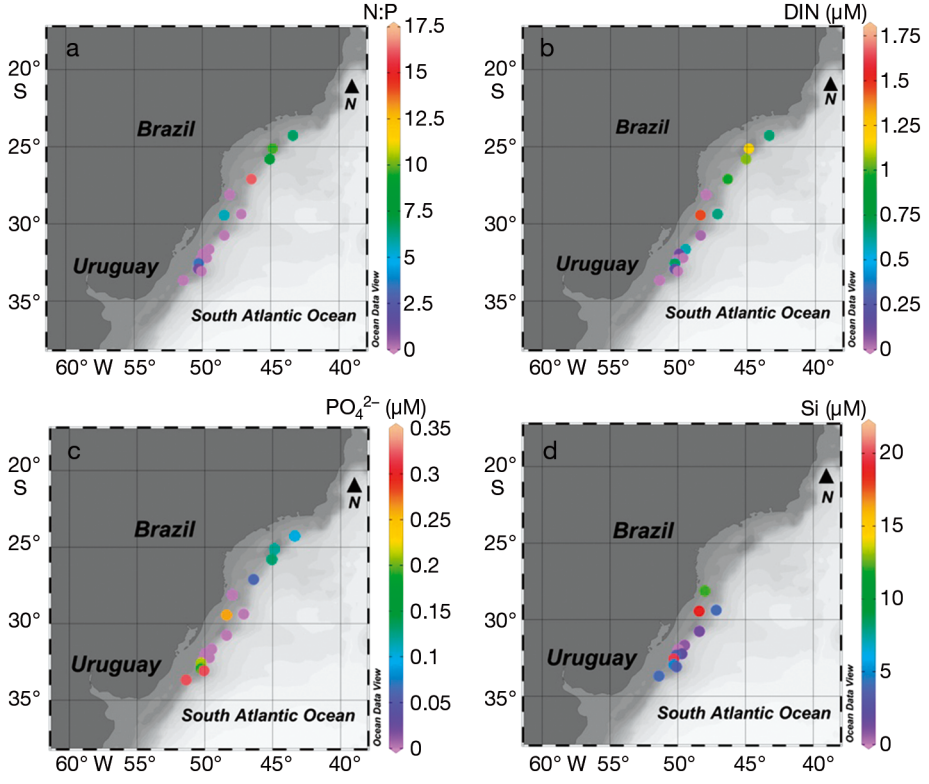

Fig. 3. Concentration of nutrients at the surface of the South Atlantic Ocean, showing (a) N:P ratio, (b) dissolved inorganic nitrogen (DIN), (c) phosphate, and (d) silicate

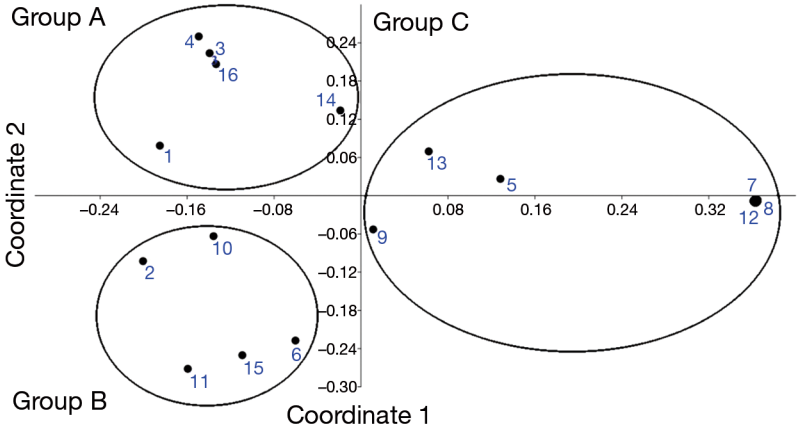

Fig. 4. nMDS ordination, dividing the sampling stations into 3 distinct groups according to the *Trichodesmium* organization: Group A, where puff-shaped colonies contribute the most to total abundance; Group B, where tuft-shaped colonies dominate; and Group C, where single trichomes account for most of the total abundance. ANOSIM revealed significant differences between the groups: $R^2 = 0.69$, stress = 0.045 (<0.5)

depths are shown in Figs. 5 & 6 (for the northern- and southernmost stations, respectively). The highest abundances of *Trichodesmium*, both as colonies and single trichomes, were found above 50 m. The figures are divided as northern and southern plots for a better visualization of the abundance, since the northern samples were more concentrated. Following the same pattern of *Trichodesmium* abundance at the surface (Fig. 2), the vertical profiles of trichomes versus depth were orders of magnitudes higher in the northern samples than in the southern stations.

Each vertical profile was integrated in order to verify the contribution of the colonies to the total abundance of trichomes. The scatter plot resulted in a strong correlation between the number of colonies and total trichomes in the station, independent of the colony shape (r = 0.93 for tuft-shaped colonies versus r = 0.88 for puffs; Fig. 7).

Vertical profiles for inorganic nutrients (phosphate, DIN, and silicate) were also collected at the southern stations, to a maximum depth of 140 m (Fig. 8). The concentration of nutrients was higher at the minimum and maximum collected depths. The higher concentrations of nutrients at depth, however, could not reach the surface due to the shallow mixed layers (Table 1). Based on the concentration of nutrients in the ocean (Baumgarten et al. 2010), the area can be considered oligotrophic.

Microscopy and chemical analysis of the particles attached to the colonies

The inverted microscopy coupled with a camera provided detailed images of *Trichodesmium* colonies with attached particles of different colors and shapes, identified in both northern and southern samples.

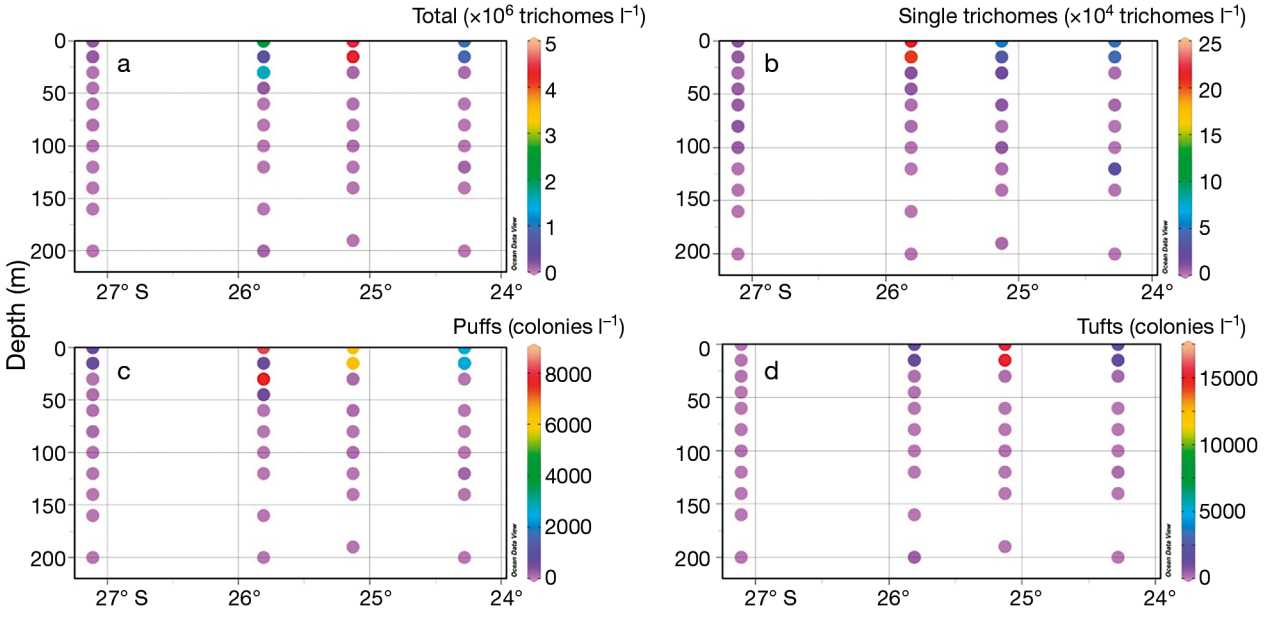

Fig. 5. Vertical distribution of *Trichodesmium* at the northernmost stations, showing (a) total trichomes l^{-1}, (b) single trichomes l^{-1}, (c) puff-shaped colonies l^{-1}, and (d) tuft-shaped colonies l^{-1}

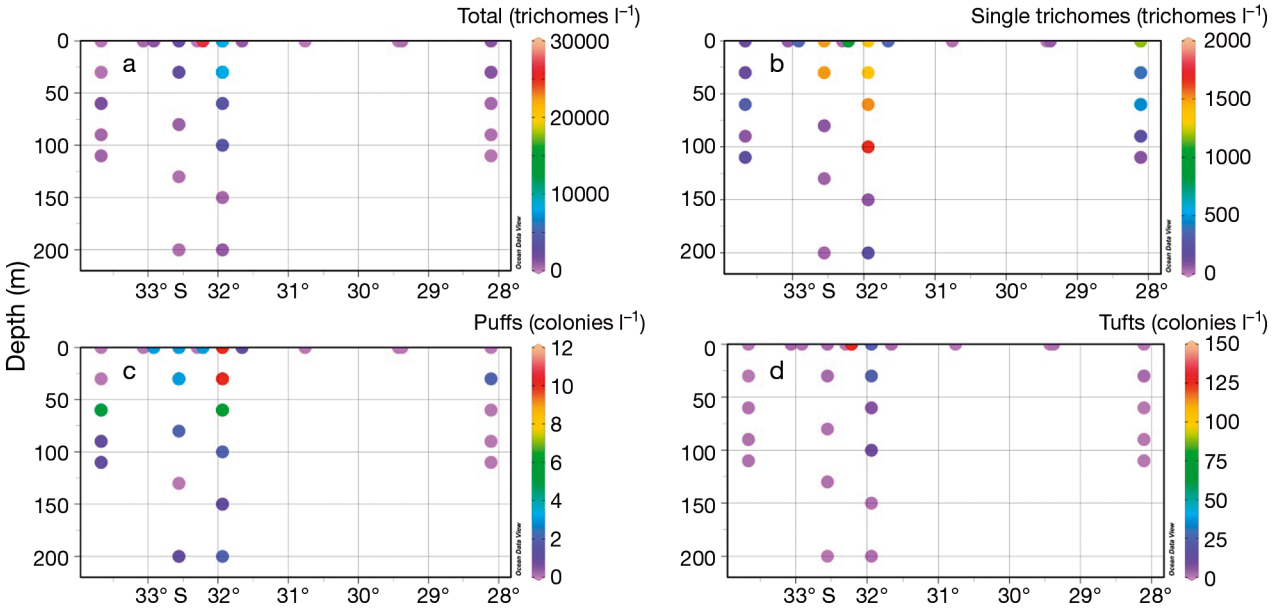

Fig. 6. As in Fig. 5, but for the southernmost stations

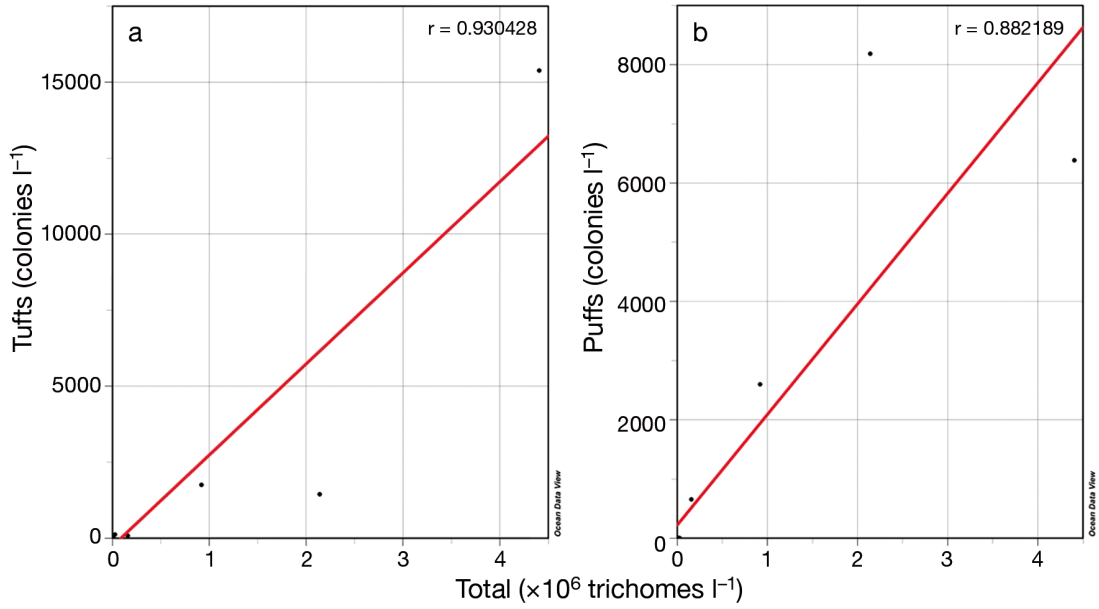

Fig. 7. Correlation between total *Trichodesmium* trichomes l^{-1} and (a) tuft-shaped colonies l^{-1} (r = 0.93) and (b) puff-shaped colonies l^{-1} (r = 0.88)

Puff-shaped colonies seemed to concentrate the particles into their center, while tufts had them spread along the trichomes (Fig. 9). These colonies were not discriminated by species; however, the trichomes and single cells were measured and had different lengths and morphological characteristics, even among colonies of the same shape. Moreover, some of the colonies were surrounded by mucilage that was preserved even after the cells were prepared for SEM analysis (see Fig. 11).

The stations analyzed by SEM coupled with EDS were chosen based on distinguishing characteristics: Stns 02 and 03 were northern stations with high abundance of colonies, Stns 09 and 10 were located at an intermediate region of the study area, and Stn 16, the southernmost station, was under the influence of the PPW. The analysis identified the range of elements and their relative contributions, as percentages, to the particle composition. Unfortunately, due to methodological constraints, the puff-shaped col-

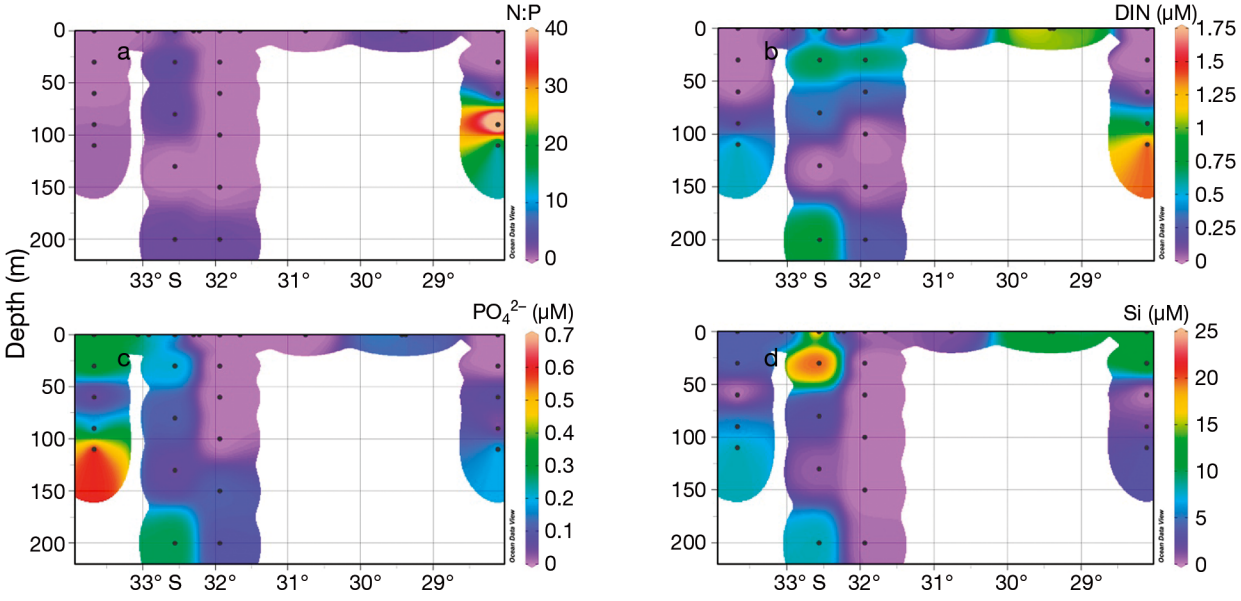

Fig. 8. Vertical distribution of nutrients at the southernmost stations, showing (a) N:P ratio, (b) dissolved inorganic nitrogen (DIN), (c) phosphate, and (d) silicate

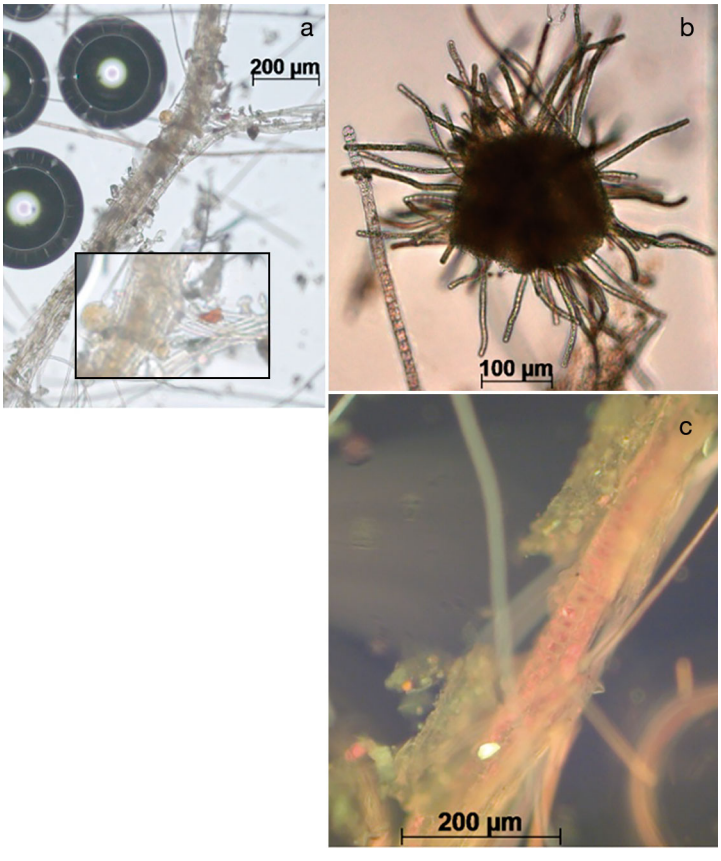

Fig. 9. Images taken by inverted microscopy (Zeiss Axiovert A1) coupled with a camera (AxioCam MRc). (a) Tuft-shaped colony with particles of different colors attached (insert shows an enlarged view). (b) Puff-shaped colony containing particles in its center. (c) Different reflectances of a particle-rich trichome; image was taken under UV light (UV fs09 ph1-04)

onies were disassembled, and we were unable to distinguish between tufts and puffs in the images. As a result, the data are shown as the average of the elemental composition of particles for each station, instead of by colony morphology (Fig. 10).

Iron (Fe) was present in particles from all stations, ranging from 12 to 29%, and phosphorus (P) and zinc (Zn) were also contained in some particles (Fig. 7). At the northernmost station analyzed (Stn 02), Fe represented 21% of the composition, P = 3% and Zn = 1%. At Stn 03, Fe contributed 12% of the average composition, followed by Zn (2%) and P (~1%). At Stn 09, Fe contributed 18% and Zn contributed 3%. At Stn 10, Fe composed 12%, while Zn contributed 5%. Finally, at the southernmost station (Stn 16), the percentage of Fe was 29% and Zn was 4%. Curiously, the southern Stns 09 and 16 contained titanium (Ti) (6 and 5%, respectively).

The SEM observations also provided detailed images of the particles (Fig. 11). Some of them could be identified as being of biogenic origin, represented by frustules (Fig. 11a). The mucilage along some of the trichomes (Fig. 11c) was analyzed by EDS and had elements in common with the particles (data not shown). Associations with bacteria, which were previously observed in *Trichodesmium* populations but have never been correlated with particles, are shown in Fig. 11d.

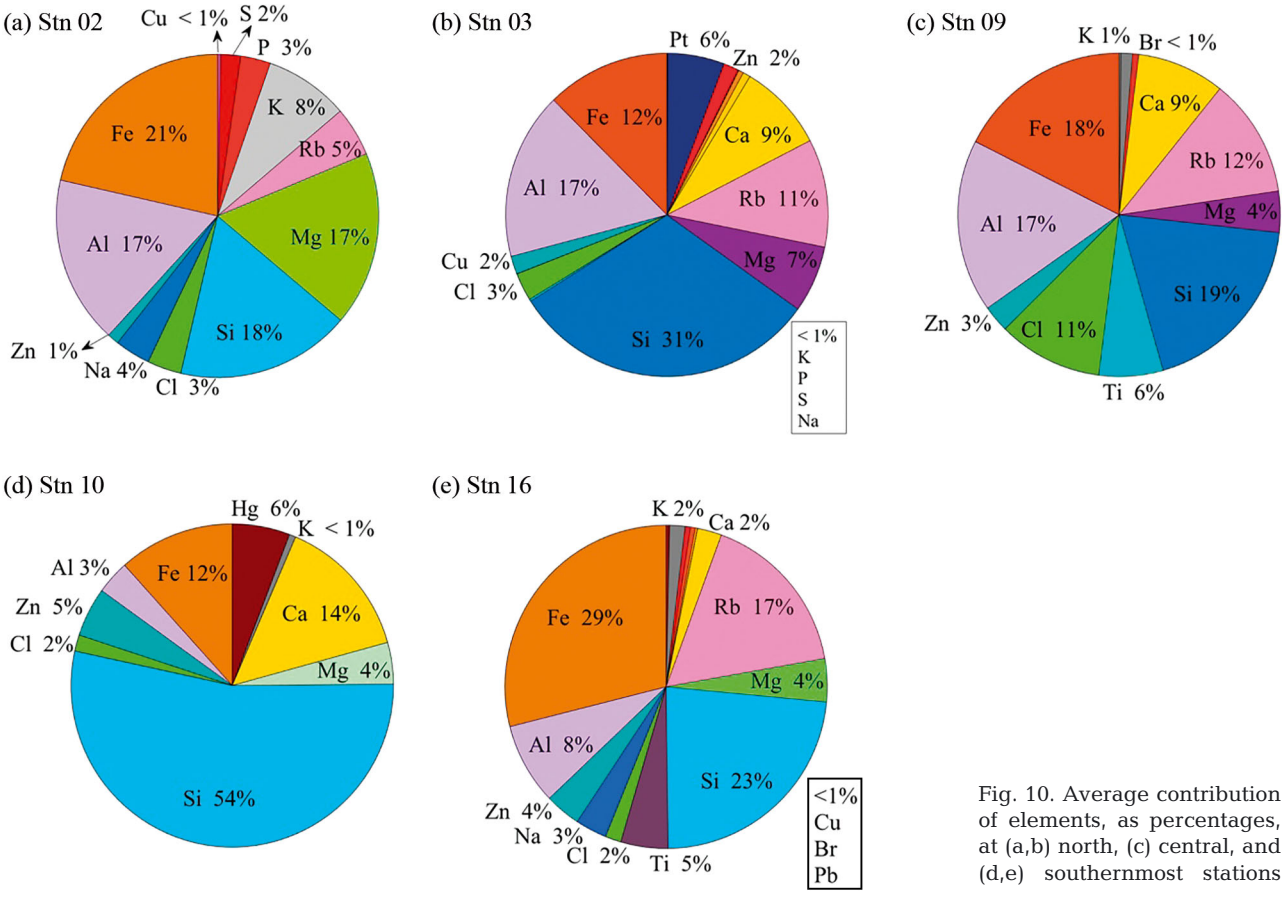

Fig. 10. Average contribution of elements, as percentages, at (a,b) north, (c) central, and (d,e) southernmost stations

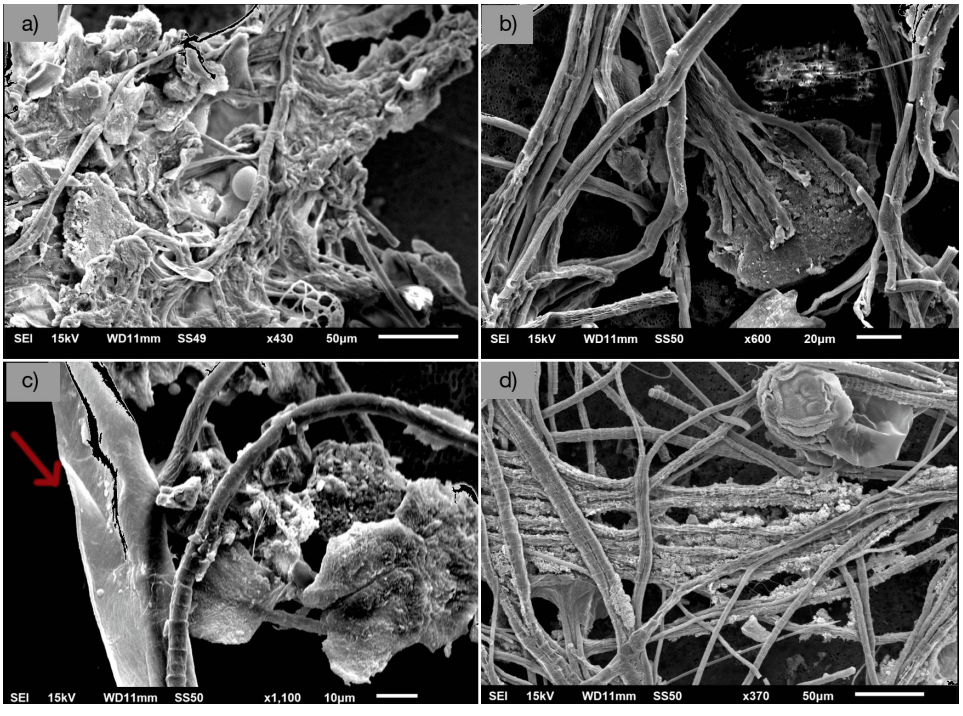

Fig. 11. SEM images of *Trichodesmium* and associated particles. (a) Details of the diversity of particles attached to the trichomes, including from biogenic origin. (b) Particle attached to trichomes. (c) Trichome with mucilage (red arrow) and particles nearby. (d) Associations between *Trichodesmium* and heterotrophic bacteria

DISCUSSION

The stations were under the influence of different water masses in the upper 200 m. Most stations were affected by TW, with the exceptions of Stns 08 and 10, which were under the influence of STSW, and Stns 13 and 16, affected by PPW (Fig. 1). The colder and less saline PPW affected 2 of the southernmost stations, the shallowest and closest to the Brazilian continental shelf (Table 1).

The abundance of *Trichodesmium* in the region decreased southwards (Table 2, Fig. 2) and with depth (Figs. 5 & 6). A previous study that focused on the northern Brazilian shelf slope found abundances of *Trichodesmium* ranging from 1000 to 1700 trichomes l^{-1} at the surface, which decreased to 100 trichomes l^{-1} at depth (Monteiro et al. 2012). These values are comparable to those from the Stns 05 to 16. In contrast, the northernmost stations were orders of magnitude higher, peaking at 2.1×10^6 trichomes l^{-1} at Stn 03. The nMDS analysis divided the stations into groups, according to the major contribution of free trichomes or colonies to the total abundance at the surface, and found no pattern between latitude or tuft/puff/single trichomes versus total trichomes l^{-1} (Fig. 4). However, when we integrated abundance along the water column and correlated it with total trichomes, colonies contributed significantly to total abundance at the stations ($r = 0.93$ for tufts and $r = 0.88$ for puffs; Fig. 7).

The concentrations of DIN (<1.5 µM) and dissolved phosphorus (<0.35) in the region were lower at the surface (Figs. 2 & 3) and slightly increased below 100 m depth in some regions (Fig. 8). However, the vertical distribution of *Trichodesmium* did not show a vertical migration for nutrient acquisition, as previously documented for other regions (Villareal & Carpenter 2003). Instead, *Trichodesmium* were preferentially distributed above the MLD, which reached 80 m at Stns 04 and 08, and <47 m at the other stations. The region of study presented N:P ratios that were equal to or below the Redfield ratio 16:1 (Table 2), which also suggests that the environment was not limited by inorganic phosphorus. The 4 northernmost stations had the highest abundances of *Trichodesmium* and N:P ratios, although they were still below the Redfield number. However, the ratios were not statistically correlated with the abundance of the organisms; instead, the highest numbers of trichomes were found in association with TW, which flows southward (Möller et al. 2008) (see Fig. 1 and Table 2).

Iron is another limiting nutrient for *Trichodesmium* growth. Unfortunately, we were not able to analyze iron concentrations in the water, and there are no previous records of this element for the region. However, the particles attached to the colonies (Fig. 9) were analyzed by EDS, and revealed high concentrations of iron at all stations, becoming a potential source of the element to the colonies (Fig. 10). The particle attachment was observed before, although not detailed, in the North Atlantic Ocean, where the organism trapped iron-rich particles from the Sahara Desert (Rueter et al. 1992). This constant Aeolian input maintains *Trichodesmium* growth in the region when combined with seasonal phosphate availability (Sañudo-Wilhelmy et al. 2001, Fernández et al. 2013). The transformation of iron-oxide dust into reduced bioavailable forms has been described under controlled laboratory conditions (Rubin et al. 2011); however, iron remineralization requires an association with heterotrophic bacteria (Roe et al. 2012). Our results show that the particle acquisition process and association with bacteria are combined in the environment, suggesting that *Trichodesmium* colonies use the particles as a source of iron (Fig. 10) and associate with heterotrophic bacteria for dissolution (Fig. 11d). Moreover, some stations had particles enriched with phosphorus and zinc, the latter composing enzymes that remove reactive oxygen species linked to oxidative stress (Howard & Rees 1996, Nuester et al. 2012). Since both elements follow the same dissolution process as iron, they could potentially be acquired in the remineralization process.

The SEM provided details on the particles attached to the colonies (Fig. 11). Fig. 11c shows mucilage produced by a trichome, a feature previously observed in *Trichodesmium* (Berman-Frank at al. 2007). To make sure that the mucilage was not an artifact originating from sample preparation, we followed the methodology required for SEM analysis using a benthic filamentous cyanobacterium from the Patos Estuary, and the sample did not present this structure. The mucilage probably acts as a mechanism to facilitate the transportation of nutrients along the trichome; however, additional studies should be carried out in order to understand its role.

High concentrations of Ti at Stns 09 and 16 served as a tracer for the source of particles at the southernmost stations. Although Stn 09 was not directly influenced by the PPW by the time the samples were collected (Fig. 1), the La Plata River plume constantly reaches the region, especially during the autumn and winter (Burrage et al. 2008). The La Plata basin system is one of the largest in the world

and, for comparison, exceeds 25% of the total discharge of the Mississippi River (USA). The system covers parts of Brazil, Bolivia, Argentina, Paraguay, and Uruguay, and the Paraná and Uruguay Rivers are the most important tributaries (Berbery & Barros 2002). These 2 rivers carry heavy metals in their waters and are enriched in Ti (Depetris & Pasquini 2007). A geochemical analysis of the sediments from the platform that are associated with PPW showed significant concentrations of amphiboles (Campos et al. 2008), minerals that can be enriched by both Fe and Ti during the crystallization process (Salminen et al. 2005).

SUMMARY

Populations of *Trichodesmium* were found in the southwestern Atlantic Ocean at different abundances, decreasing southwards and with depth. They were organized as single trichomes or in colonies with different morphologies, characterized as puffs and tufts. The surface waters in the study area contained low nutrient concentrations, but were not limited by phosphate. We observed colonies of *Trichodesmium* with particles attached to their surface and interior that were composed of a wide range of elements, especially the nutrients iron, phosphorus, and zinc. SEM images also identified an association between the colonies and bacteria that contribute to the dissolution of the particle compounds into more bioavailable species. In the southernmost region, the La Plata River input was an important source of sediments containing iron. Finally, the South Atlantic Ocean needs to be further investigated in order to explain the interactions between *Trichodesmium* and the environment, especially N_2 fixation rates that were not addressed in this work. However, this study provided a detailed analysis of vertical and spatial distribution of *Trichodesmium* in the region; an adaptation for nutrient acquisition involving autotroph–heterotroph association and particle aggregation; and a potential source of nutrients in the southern region of study.

Acknowledgements. We thank the TALUDE project, granted by Chevron®, for the opportunity to collect samples during their cruises on the Brazilian RV 'Atlântico Sul.' We are also grateful to the CEME-Sul Center of Microscopy for facilitating the SEM analysis coupled with EDS. Finally, we thank technician Edi Morales Jr. for assistance with the nutrient analysis. M.B.B. was funded by an MSc grant fellowship from CAPES – Brazil.

LITERATURE CITED

Agawin NS, Tovar-Sánchez A, de Zarruk KK, Duarte CM, Agustí S (2013) Variability in the abundance of *Trichodesmium* and nitrogen fixation activities in the subtropical NE Atlantic. J Plankton Res 35:1126–1140

Aminot A, Chaussepied M (1983) Manuel des analyses chimiques en milieu marin. Centre National pour L'Exploitation des Oceans, Brest

Baumgarten MDGZ, de Barros Rocha JM, Niencheski LFH (2010) Manual de análises em oceanografia química. Universidade Federal do Rio Grande, Rio Grande

Berbery EH, Barros VR (2002) The hydrologic cycle of the La Plata Basin in South America. J Hydrometeorol 3: 630–645

Berman-Frank I, Rosenberg G, Levitan O, Haramaty L, Mari X (2007) Coupling between autocatalytic cell death and transparent exopolymeric particle production in the marine cyanobacterium *Trichodesmium*. Environ Microbiol 9:1415–1422

Bray JR, Curtis JT (1957) An ordination of the upland forest communities of Southern Wisconsin. Ecol Monogr 27: 325–349

Burrage D, Wesson J, Martinez C, Pérez T, Möller O Jr, Piola A (2008) Patos Lagoon outflow within the Río de la Plata plume using an airborne salinity mapper: observing an embedded plume. Cont Shelf Res 28:1625–1638

Campos EJ, Mulkherjee S, Piola A, Carvalho FMS (2008) A note on a mineralogical analysis of the sediments associated with the Plata River and Patos Lagoon outflows. Cont Shelf Res 28:1687–1691

Capone DG, Burns JA, Montoya JP, Subramaniam A and others (2005) Nitrogen fixation by *Trichodesmium* spp.: an important source of new nitrogen to the tropical and subtropical North Atlantic Ocean. Global Biogeochem Cycles 19:GB2024

Carpenter EJ (1983) Nitrogen fixation by marine Oscillatoria (*Trichodesmium*) in the world's oceans. In: Carpenter EJ, Capone DG (eds) Nitrogen in the marine environment. Elsevier, New York, NY, p 65–103

Carpenter EJ, Price CC (1976) Marine Oscillatoria (*Trichodesmium*): explanation for aerobic nitrogen fixation without heterocysts. Science 191:1278–1280

Carvalho M, Gianesella SM, Saldanha-Corrêa FM (2008) *Trichodesmium erythraeum* bloom on the continental shelf off Santos, Southeast Brazil. Braz J Oceanogr 56: 307–311

Clarke KR (1993) Non-parametric multivariate analyses of changes in community structure. Aust J Ecol 18:117–143

Cronberg G, Carpenter EJ, Carmichael WW (2003) Taxonomy of harmful cyanobacteria. In: Hallegraeff GM, Anderson DM, Cembella AD (eds) Manual on harmful marine microalgae. UNESCO Publishing, Paris, p 523–562

Depetris PJ, Pasquini AI (2007) The geochemistry of the Paraná River: an overview. In: Iriondo MH, Paggi JC, Parma MJ (eds) The Middle Paraná River: limnology of a subtropical wetland. Springer, Berlin, p 143–174

Fernández A, Graña R, Mouriño-Carballido B, Bode A, Varela M, Domínguez-Yanes JF, Marañón E (2013) Community N_2 fixation and *Trichodesmium* spp. abundance along longitudinal gradients in the eastern subtropical North Atlantic. ICES J Mar Sci 70:223–231

Hammer O, Harper DAT, Ryan PD (2008) PAST — PAlaeontological STatistics, Ver. 1.81. http://folk.uio.no/ohammer/past

Ho TY (2013) Nickel limitation of nitrogen fixation in *Trichodesmium*. Limnol Oceanogr 58:112–120

Howard JB, Rees DC (1996) Structural basis of biological nitrogen fixation. Chem Rev 96:2965–2982

Hutchins DA, Witter AE, Butler A, Luther GW III (1999) Competition among marine phytoplankton for different chelated iron species. Nature 400:858–861

Karl D, Michaels A, Bergman B, Capone D and others (2002) Dinitrogen fixation in the world's oceans. Biogeochemistry 57/58:47–98

Komárek J, Anagnostidis K (2007) Cyanoprokaryota, II. Teil. Oscillatoriales. In: Büdel B, Krienitz L, Gärtner G, Schagerl M (eds) Süβwasserflora von Mitteleuropa. Elsevier, Munich

Koroleff F (1972) Determination of total nitrogen in natural waters by means of persulphate oxidation. In: Carlberg SR (ed) New Baltic manual with methods for sampling and analysis of physical, chemical, and biological parameters. Co-op Res Ser A-20. International Council for the Exploration of the Sea, Charlottenlund, p 73–78

LaRoche J, Breitbarth E (2005) Importance of the diazotrophs as a source of new nitrogen in the ocean. J Sea Res 53: 67–91

Luo YW, Doney SC, Anderson LA, Benavides M and others (2012) Database of diazotrophs in global ocean: abundance, biomass and nitrogen fixation rates. Earth Syst Sci Data 4:47–73

Möller OO Jr, Piola AR, Freitas AC, Campos EJD (2008) The effects of river discharge and seasonal winds on the shelf off southeastern South America. Cont Shelf Res 28: 1607–1624

Monteiro JJF, Leça EE, Koening ML, Macedo SJ (2012) Distribution and annual variation of *Trichodesmium thiebautii* Gomont Ex Gomont (Oscillatoriales - Cyanophyta) in tropical waters of northeastern Brazil (Western Atlantic). Trop Oceanogr 40:319–326

Nuester J, Vogt S, Newville M, Kustka AB, Twining BS (2012) The unique biogeochemical signature of the marine diazotroph *Trichodesmium*. Front Microbiol 3:150

Paerl HW, Bebout BM (1992) Oxygen dynamic in *Trichodesmium* spp. dynamics. In: Carpenter EJ, Capone DG, Rueter JG (eds) Marine pelagic cyanobacteria: *Trichodesmium* and other diazotrophs. Springer, Dordrecht, p 43–60

Roe KL, Barbeau K, Mann EL, Haygood MG (2012) Acquisition of iron by *Trichodesmium* and associated bacteria in culture. Environ Microbiol 14:1681–1695

Rubin M, Berman-Frank I, Shaked Y (2011) Dust- and mineral-iron utilization by the marine dinitrogen-fixer *Trichodesmium*. Nat Geosci 4:529–534

Rueter JG, Hutchins DA, Smith RW, Unsworth NL (1992) Iron nutrition of *Trichodesmium*. In: Carpenter EJ, Capone DG, Rueter JG (eds) Marine pelagic cyanobacteria: *Trichodesmium* and other diazotrophs. Springer, Dordrecht, p 289–306

Salminen R, Batista MJ, Bidovec M, Demetriades A and others (2005) Geochemical Atlas of Europe. Part 1 — Background information, methodology and maps. Geological Survey of Finland, Otamedia Oy, Espoo

Sañudo-Wilhelmy SA, Kustka AB, Gobler CJ, Hutchins DA and others (2001) Phosphorus limitation of nitrogen fixation by *Trichodesmium* in the central Atlantic Ocean. Nature 411:66–69

Sato S, Paranaguá MN, Eskinazi E (1963) On the mechanism of red tide of *Trichodesmium* in Recife northeastern Brazil, with some considerations of the relation to the human disease, 'Tamandare fever'. Trab Inst Oceanogr Univ Recife 5:7–49

Sohm JA, Capone DG (2006) Phosphorus dynamics of the tropical and subtropical north Atlantic: *Trichodesmium* spp. versus bulk plankton. Mar Ecol Prog Ser 317:21–28

Tyrrell T, Marañón E, Poulton AJ, Bowie AR, Harbour DS, Woodward EMS (2003) Large-scale latitudinal distribution of *Trichodesmium* spp. in the Atlantic Ocean. J Plankton Res 25:405–416

Utermöhl H (1958) Zur Vervollkommnung der quantitativen Phytoplankton-Methodik. Mitt Int Ver Theor Angew Limnol 9:1–38

Villareal TA, Carpenter EJ (2003) Buoyancy regulation and the potential for vertical migration in the oceanic cyanobacterium *Trichodesmium*. Microb Ecol 45:1–10

Editorial responsibility: Douglas Capone, Los Angeles, California, USA

Submitted: July 7, 2016; Accepted: November 23, 2016
Proofs received from author(s): January 18, 2017